Coupled COAMPS Extended Range MJO Prediction

PI: Sue Chen
Naval Research Laboratory
Monterey, CA 93943-5502
Phone: (831) 656-4737, fax: (831) 656-4769, e-mail: sue.chen@nrlmry.navy.mil

Co-PI: James D. Doyle
Naval Research Laboratory
Monterey, CA 93943-5502
Phone: (831) 656-4716, fax: (831) 656-4769, e-mail: james.doyle@nrlmry.navy.mil

Co-PI: Paul May
Computer Sciences Corporation
Monterey, CA 93943-5502
Phone: (831) 656-4706, fax: (831) 656-4769, e-mail: paul.may@nrlmry.navy.mil

Co-PI: Jerome M. Schmidt
Naval Research Laboratory
Monterey, CA 93943-5502
Phone: (831) 656-4702, fax: (831) 656-4769, e-mail: Jerome.schmidt@nrlmry.navy.mil

Award Number: N0001412WX21508

LONG-TERM GOALS

The Madden Julian Oscillation (MJO) influences the intraseasonal variability in the tropics. It is essential to understand factors that contribute to the model forecast errors associated with the extended prediction of the MJO. The long-term goals of this research are to identify the physical processes that affect the extended range prediction of the MJO and shed light on future improvements in the model parameterizations and ensemble forecast strategies that aim to increase the seasonal prediction skill of the NAVY models.

OBJECTIVES

The objectives of this project are to use a fully coupled COAMPS to investigate the effect of air-ocean coupling, the prediction barrier problem near the Maritime Continent, and cloud-resolving impact on the MJO structure. There are some indications that air-sea coupling improved the MJO prediction but the mechanisms are not well understood. Many coupled and uncoupled global seasonal prediction models as well as global NWP models have a low skill in forecasting the MJO propagation from the Indian Ocean to the Maritime Continent. Does the lack of model horizontal resolution, or model parameterizations of air-sea coupling, or parameterizations of convection, or all of these factors contribute to this prediction barrier?

Report Documentation Page

Form Approved
OMB No. 0704-0188

1. REPORT DATE **SEP 2012**	2. REPORT TYPE	3. DATES COVERED **00-00-2012 to 00-00-2012**
4. TITLE AND SUBTITLE **Coupled COAMPS Extended Range MJO Prediction**		5a. CONTRACT NUMBER 5b. GRANT NUMBER 5c. PROGRAM ELEMENT NUMBER
6. AUTHOR(S)		5d. PROJECT NUMBER 5e. TASK NUMBER 5f. WORK UNIT NUMBER
7. PERFORMING ORGANIZATION NAME(S) AND ADDRESS(ES) **Naval Research Laboratory,7 Grace Hopper Avenue,Monterey,CA,93943-5502**		8. PERFORMING ORGANIZATION REPORT NUMBER
9. SPONSORING/MONITORING AGENCY NAME(S) AND ADDRESS(ES)		10. SPONSOR/MONITOR'S ACRONYM(S) 11. SPONSOR/MONITOR'S REPORT NUMBER(S)
12. DISTRIBUTION/AVAILABILITY STATEMENT **Approved for public release; distribution unlimited**		
13. SUPPLEMENTARY NOTES		
14. ABSTRACT		
15. SUBJECT TERMS		

16. SECURITY CLASSIFICATION OF:			17. LIMITATION OF ABSTRACT	18. NUMBER OF PAGES	19a. NAME OF RESPONSIBLE PERSON
a. REPORT	b. ABSTRACT	c. THIS PAGE			
unclassified	**unclassified**	**unclassified**	**Same as Report (SAR)**	**9**	

Standard Form 298 (Rev. 8-98)
Prescribed by ANSI Std Z39-18

APPROACH

The sensitivity of the MJO characteristics to air-ocean coupling processes will be explored by performing low-resolution (45 km in the atmosphere and ocean) coupled, one-way coupled, and uncoupled runs. We will use a 15 km set up and a 15/5 km moving nest version that follows the propagation of the MJO in the coupled and uncoupled versions of COAMPS to see how the horizontal resolution and model representation of convection impacts the MJO as it passes through Sumatra. We will analyze the structure of the convective heating rate from the 45/15 km (convective parameterization) and 5 km (cloud resolving) coupled and uncoupled runs to examine the impact of parameterized convection on the extended MJO forecasts.

The model coarse resolution domain will be setup large enough such that the use of analysis lateral boundary conditions from NOGAPS and global NCOM will not contaminate the model solution in Indian Ocean over the 15-20 day period. We will compare and contrast the extended range predictions and observed MJOs captured during the CINDY/DYNAMO/AMI/LASP campaign. High frequency DYNAMO soundings as well as other relevant in-situ observations will be used to validate these model sensitivity runs.

WORK COMPLETED

We completed a series of 15-day simulations on the second CINDY/DYNAMO MJO case observed on Nov 24, 2011. The simulations consist of seven 45 km and one 15 km resolution runs that covers area from 30°S to 30°N and from 23°W to 102°W (Fig. 1). The control run (RUN1) is an uncoupled simulation initialized on 0000UTC 20 Oct with analyzed NCODA SST and atmospheric data assimilation. The SST is fixed throughout the 15-day model integration. RUN2 is similar to the control except the SST is updated daily using the global NCODA analysis SST. RUN3 is a one-way coupled experiment that uses the NCOM SST at the initial time. The SST does not feedback to the atmosphere. RUN4 is a fully coupled air-ocean run and the SST feedback to the atmosphere occurs every 6 min.

RUN5-7 are identical to RUN1-3 except we initialized the model at 1200 UTC when the diurnal SST was near its daily maximum on 20 Oct. The main purpose of RUN5-7 is to investigate the impact of a fully charged ocean on the MJO phase and propagation speed. RUN8 is similar to RUN7 except it is at 15 km resolution. A summary of the sensitivity experiments that have been completed is listed in table 1.Preliminary analysis of the numerical experiments RUN1-3 and comparison with TRMM precipitation was presented at the July 2012 ONR LASP DRI workshop.

Table 1: List of COAMPS experiments

Experiment Name	Descriptions
RUN1	Uncoupled 45 km, initialized on 0000 UTC, NCODA SST
RUN2	One-way coupled 45 km, initialized on 0000 UTC, NCODA SST
RUN3	Uncoupled 45 km, initialized on 0000 UTC, gNCOM SST
RUN4	Two-way coupled 45 km, initialized on 0000 UTC
RUN5	Uncoupled 45 km, initialized on 1200 UTC
RUN6	One-way coupled 45 km, initialized on 1200 UTC
RUN7	Two-way coupled 45 km, initialized on 1200 UTC
RUN8	Two-way coupled 15 km, initialized on 1200 UTC

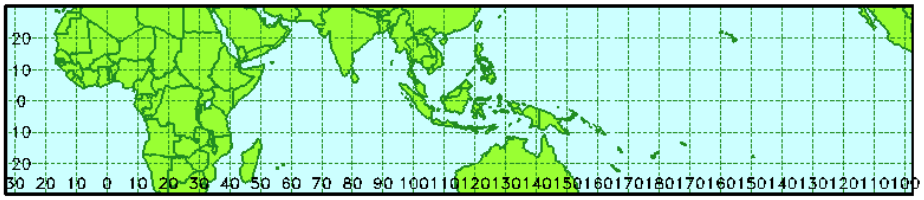

Fig. 1 Area map of COAMPS 45 km model domain.

RESULTS

One of the main hypotheses proposed by the related ONR LASP DRI “Coupled MJO project” was that the initiation of the second MJO observed during CINDY/DYNAMO resulted from a phase-locking and contraction of the Kelvin and Rossby waves. To further examine the extended prediction of this phenomena, we employed a two-dimensional space and time FFT filtering technique (Dr. Maria Flatau, personal communication) to remove the diurnal high frequency signal from the observed and model precipitation data and separate the signals associated with the eastward and westward propagating waves, The precipitation is used as a proxy to evaluate the prediction and propagation of the MJO. The eastward moving waves include the MJO and Kelvin waves and the westward moving waves include the inertial gravity, Rossby, and mixed Rossby-Gravity waves.

Fig.2 shows the Hovmöller diagram of 5°S-5°N FFT and band pass filtered 3 hourly precipitation derived from three coupled COAMPS forecasts and from 0.25° TRMM satellite. TRMM observations show two eastward propagating modes originated around 22 and 26 Nov between 60-80°E. The first mode represents the initiation of MJO in the central Indian Ocean (IO). The second mode forms behind the first mode, which eventually crosses the Maritime Continent to the Western Pacific. The first mode is also associated with the passage of a Kelvin wave. These two eastward propagating modes are captured in the 45 km coupled RUN4 (0000UTC) and RUN7 (1200UTC) but both runs have a much weaker magnitude compared to TRMM and 15 km RUN8. Interestingly, RUN7 produces stronger eastward propagating modes than RUN4, indicating more energy in the eastward propagating modes when COAMPS is initiated during the warm phase of diurnal SST cycle (1700 LT). This result suggests that when designing an ensemble seasonal prediction system, consideration of members that are initialized at different phases of the diurnal heating cycle may allow for a wider range of uncertainty and increase the ensemble spread.

Among three coupled COAMPS forecasts, RUN8 (15 km) produces stronger eastward propagating modes than lower resolution 45 km RUN4 and RUN7. Overall we noticed RUN8 has more convective (sub-grid scale) and stable (grid-scale) precipitation over the ocean than RUN 7. However the magnitudes of these two modes produced by RUN8 are still weaker than TRMM, suggesting a bias in the magnitude of MJO convection in RUN8. There are several possible causes that may create this bias including not enough large-scale convergence or local air-sea fluxes into the convective region. Further examination of the wind fields suggest a weaker westerly wind burst at the equator in RUN8 may contribute to the weaker convective signals.

All three coupled COAMPS runs have much stronger westward propagating modes than the eastward modes and agree well qualitatively with the TRMM. COAMPS shows two distinctive westward propagating modes while the second mode in TRMM is weaker than COAMPS (Fig. 3). In COAMPS, the first westward mode is from the passage of a Rossby wave on 24 Nov and the second mode does

not travel as far west as the first mode. It ends around 80°E around 28 Nov. In TRMM, instead of two modes seen in COAMPS, there is a single broader envelop of westward propagation that can be traced back from the Western Pacific around 140°E and end around 70°E on 28 Nov. Again the 15 km RUN8 has the strongest westward modes than the 45 km RUN4 and RUN7.

The influence of coupling is seen in the analysis of RUN1-RUN2 and RUN3-RUN4 pairs of experiments. The first pair uses the analyzed SST from NCODA so we can minimize the SST bias to examine the coupling effect. The second pair uses forecast SST from NCOM. RUN2 is an analog to a 1-way coupled simulation since we update the SST once a day. We repeat the experiment using an initial condition from daytime to see whether the coupling effect seen in the first pair of experiments is the same as in the second pair of experiments. Our results show for the eastward propagating mode, the uncoupled runs have more precipitation over land than the coupled runs. Over the ocean, the coupled and uncoupled runs are very similar. However, the coupled run has a slightly stronger first MJO mode than the uncoupled run. The initiation of the second MJO mode is delayed about a day in the uncoupled run and the coupled run has a stronger MJO signal in the Western Pacific (Fig. 4). The results from the 1200UTC runs are similar to the 0000UTC runs.

For the westward propagating modes (5°N-10°N), the main difference between the coupled and uncoupled 0000UTC runs is the phase of propagation and the amplitude of the anomaly. The uncoupled run starts the westward propagation about half of day earlier than the two-way coupled run. While for the uncoupled and one-way coupled NCODA SST runs, the uncoupled runs have a larger magnitude than the one-way coupled runs (Fig. 5).

The close coupling of atmosphere and ocean in COAMPS should permit us to examine and test various mechanisms by which the MJO signal is transmitted along the equatorial waveguide and communicated back and forth between the two mediums. Fig. 6 is a Hovmoller plot of sea temperature along the equator at 100m, the approximate depth of the seasonal thermocline, that shows an eastward propagating warm feature whose speed is about that of a first mode baroclinic Kelvin wave. This feature originates in the eastern Indian Ocean and arrives in mid-Indian ocean very near to the initiation of the MJO event. The nature of the propagating warm ocean feature and hard evidence of the association of oceanic and atmospheric events requires further analysis.

In summary, the 45 km coupling experiments show the effects of coupling are to delay the westward propagating Rossby modes and enhance the eastward propagating MJO mode. However the eastward modes are much weaker than the westward modes in the 45km simulations. The eastward modes in the higher-resolution 15km coupled run are stronger than the 45km runs and are closer to the TRMM observations. Even with a stronger eastward mode in the 15km run, the second MJO mode is still weaker than TRMM. This second MJO mode is related to weaker westerly wind burst at the equator. We are performing additional calculations and sensitivity experiments to sort out what causes this prediction barrier in COAMPS. We also found initializing COAMPS during daytime hours produces better eastward propagating modes. This result suggests it may be important to include ensemble members that are initialized at different times in the diurnal cycle to increase the ensemble spread. The exact nature of the coupling between ocean and atmosphere is unclear at this point but the coupled model shows potential for elucidating the mechanisms by some careful analysis of additional experiments.

IMPACT/APPLICATIONS

We have examined the impact of coupling on the evolution and propagation of extended MJO forecast and have made progress toward identifying the physical processes that are responsible for these differences. The successful completion of this project will provide insight into improving the model parameterizations that are crucial to increasing the MJO forecast skill and configuration of the ensemble system for seasonal prediction. Knowledge learned from this project can potentially benefit projects related to improving the seasonal prediction skill of limited and global models.

RELATED PROJECTS

This project is closely related to a number of ONR programs on "Coupled MJO", "Impact of resolution on extended-range multi-scale simulations", and "Physics parameterization for seasonal prediction".

PUBLICATIONS

Chen S., P. May, J. Doyle, M. Flatau, and J. M. Schmidt, 2012: Air-sea Interaction Influence on the MJO propagation, 3-7 Dec, San Francisco (poster).

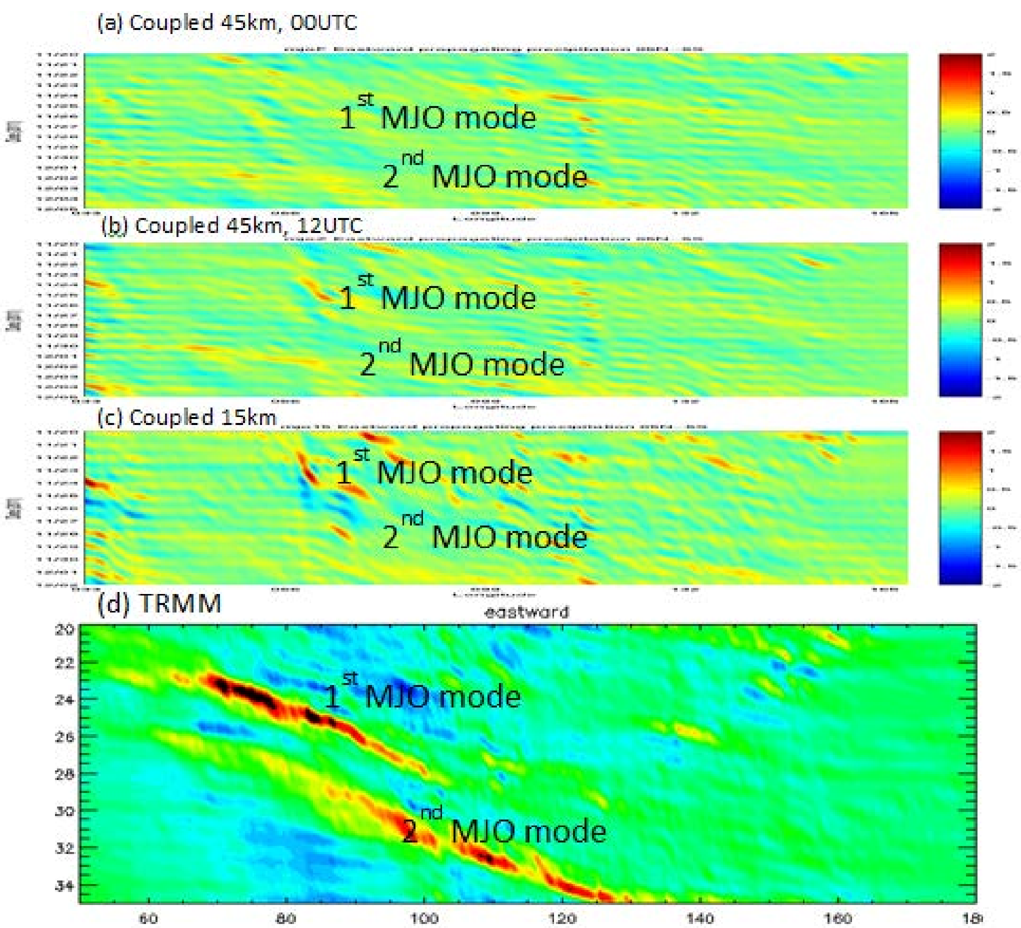

Fig. 2 Hovmöller diagram of 5°S-5°N FFT and band pass filtered eastward propagating precipitation modes from (a)-(c) 45km 00UTC, 45km 12UTC, and 15km 12UTC coupled OCAMPS simulations with respectively and (d) from TRMM.

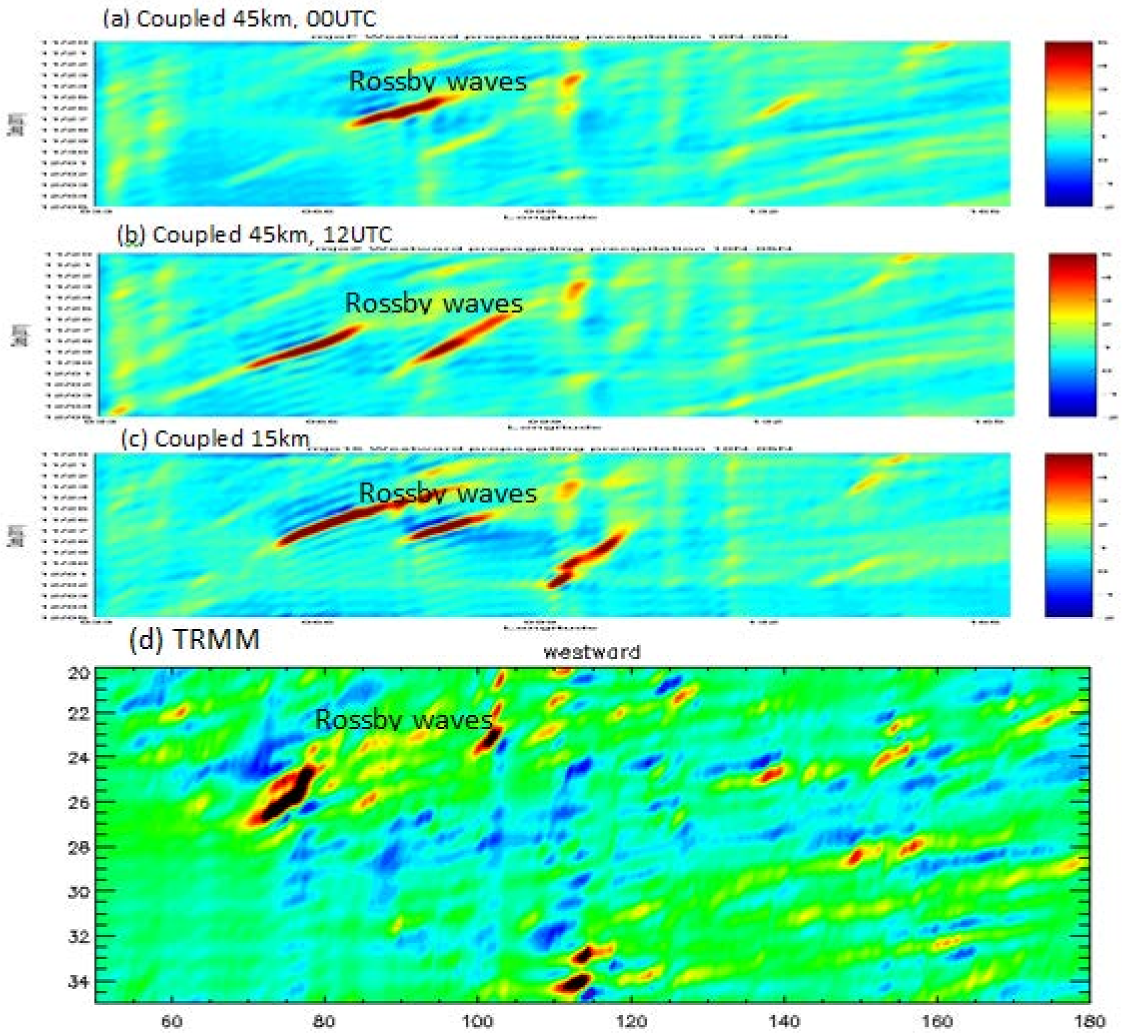

Fig. 3 Hovmöller diagram of 5°N-10°N FFT and band pass filtered westward propagating precipitation modes from (a)-(c) 45km 00UTC, 45km 12UTC, and 15km 12UTC coupled OCAMPS simulations with respectively and (d) from TRMM.

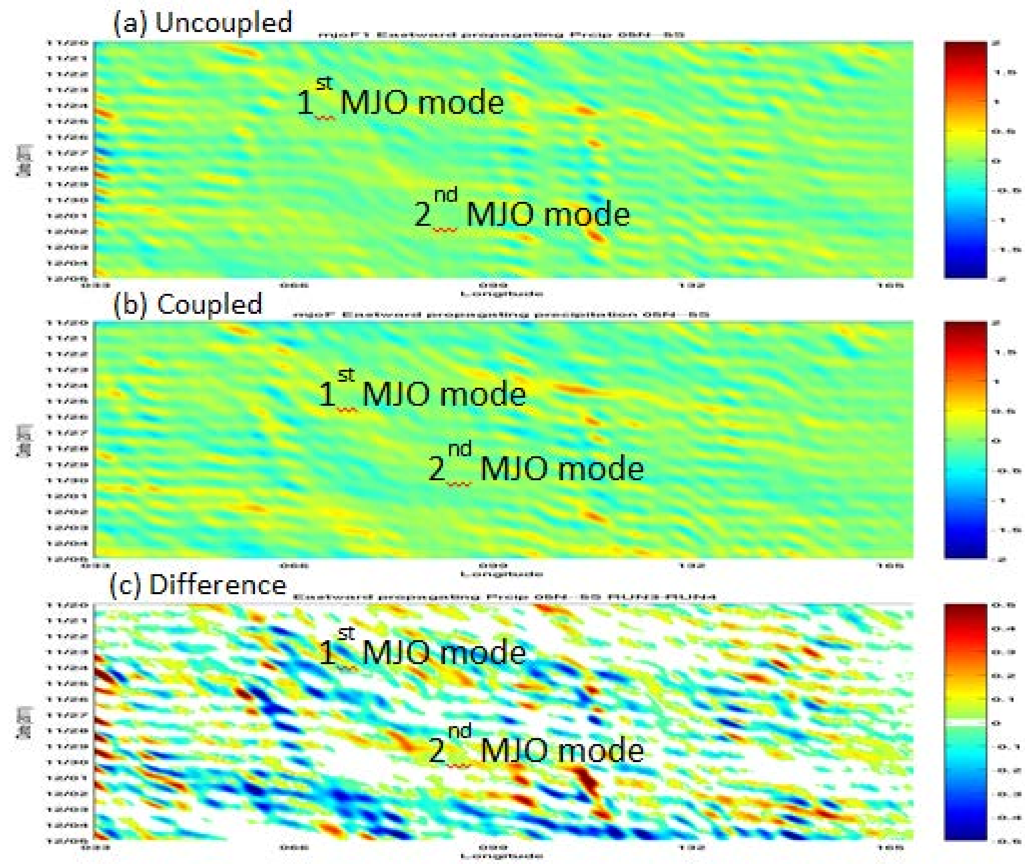

Fig. 4 Hovmöller diagram of 5°S-5°N FFT and band pass filtered eastward propagating precipitation modes from (a) uncoupled, (b) coupled, and (c) uncoupled-coupled COAMPS 45km 00TUC simulations.

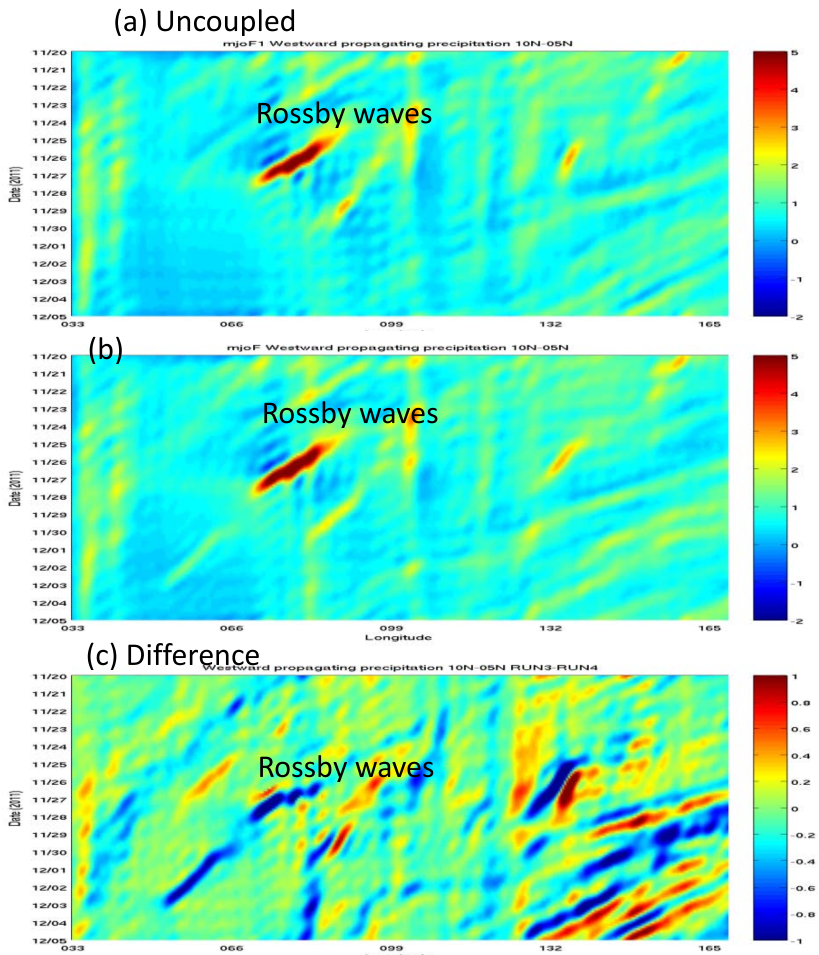

Fig. 5 Hovmöller diagram of 5°S-5°N FFT and band pass filtered westward propagating precipitation modes from (a) uncoupled, (b) coupled, and (c) uncoupled-coupled COAMPS 45km 00TUC simulations.

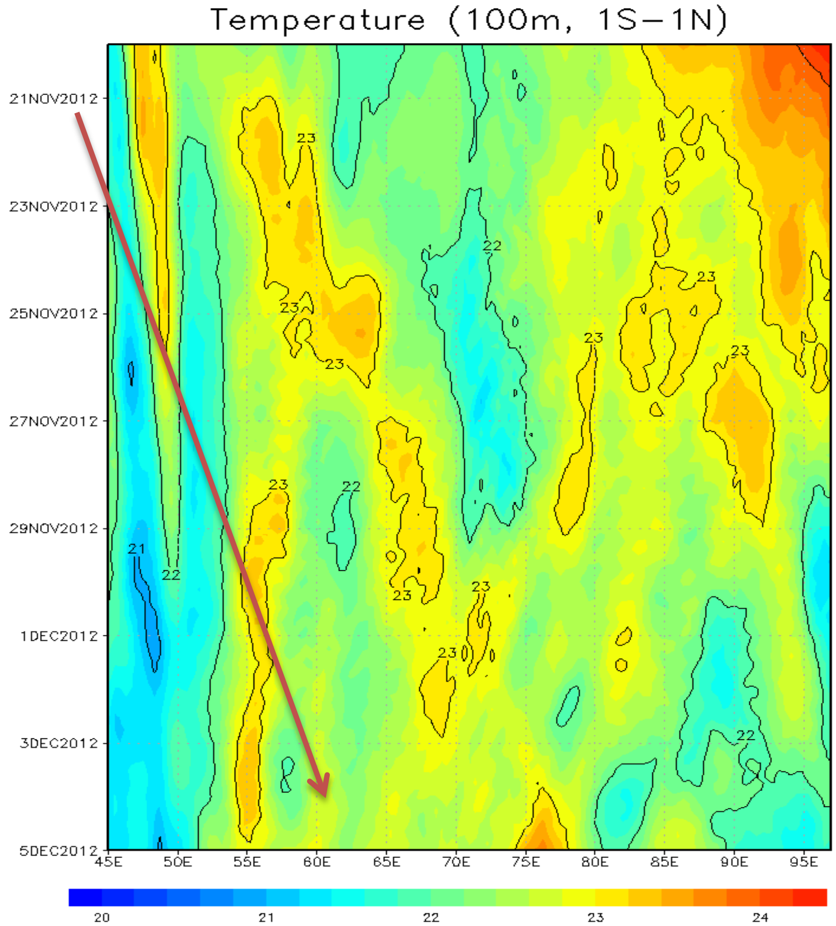

Fig. 6 Hovmöller diagram of 1°S-1°N sea temperature at 100m showing eastward propagating warm feature at the depth of the seasonal thermocline.